

# Titan's plasma environment during a magnetosheath excursion: Real-time scenarios for Cassini's T32 flyby from a hybrid simulation

S. Simon<sup>1,2</sup>, U. Motschmann<sup>1,3</sup>, G. Kleindienst<sup>4</sup>, J. Saur<sup>2</sup>, C. L. Bertucci<sup>5</sup>, M. K. Dougherty<sup>5</sup>, C. S. Arridge<sup>6</sup>, and A. J. Coates<sup>6</sup>

<sup>1</sup>Institute for Theoretical Physics, TU Braunschweig, Germany

<sup>2</sup>Institute of Geophysics and Meteorology, University of Cologne, Germany

<sup>3</sup>Institute for Planetary Research, DLR, Berlin, Germany

<sup>4</sup>Institute for Geophysics and Extraterrestrial Physics, TU Braunschweig, Germany

<sup>5</sup>The Blackett Laboratory, Imperial College, London

<sup>6</sup>Mullard Space Science Laboratory, University College, London

Received: 11 July 2008 – Revised: 6 January 2009 – Accepted: 16 January 2009 – Published: 12 February 2009

**Abstract.** With a Saturnian magnetopause average stand-off distance of about 21 planetary radii, Titan spends most of its time inside the rotating magnetosphere of its parent planet. However, when Saturn's magnetosphere is compressed due to high solar wind dynamic pressure, Titan can cross Saturn's magnetopause in the subsolar region of its orbit and therefore to interact with the shocked solar wind plasma in Saturn's magnetosheath. This situation has been observed during the T32 flyby of the Cassini spacecraft on 13 June 2007. Until a few minutes before closest approach, Titan had been located inside the Saturnian magnetosphere. During the flyby, Titan encountered a sudden change in the direction and magnitude of the ambient magnetic field. The density of the ambient plasma also increased dramatically during the pass. Thus, the moon's exosphere and ionosphere were exposed to a sudden change in the upstream plasma conditions. The resulting reconfiguration of Titan's plasma tail has been studied in real-time by using a three-dimensional, multi-species hybrid simulation model. The hybrid approximation treats the electrons of the plasma as a massless, charge-neutralizing fluid, while ion dynamics are described by a kinetic approach. In the simulations, the magnetopause crossing is modeled by a sudden change of the upstream magnetic field vector as well as a modification of the upstream plasma composition. We present real-time simulation results, illustrating how Titan's induced magnetotail is reconfigured due to magnetic reconnection. The simulations allow to determine a characteristic

time scale for the erosion of the original magnetic draping pattern that commences after Titan has crossed Saturn's magnetopause. Besides, the influence of the plasma composition in the magnetosheath on the reconfiguration process is discussed in detail. The question of whether the magnetopause crossing is likely to yield a detachment of Titan's exospheric tail from the satellite is investigated as well.

**Keywords.** Magnetospheric physics (Magnetosphere interactions with satellites and rings; Magnetosphere-ionosphere interactions) – Space plasma physics (Kinetic and MHD theory; Numerical simulation studies)

## 1 Introduction

With its extended neutral atmosphere, Titan orbits Saturn at a distance of 20.3 Saturn radii and with an orbital period of 15.95 days. Most of the time, Titan's orbit is located within the outer regions of Saturn's magnetosphere, where the moon's atmosphere and ionosphere are exposed to a flow of at least partially corotating magnetospheric plasma with a relative velocity around 120 km/s (cf. for instance Neubauer et al., 1984). The stand-off distance of Saturn's magnetopause usually varies between 20 and 27 planetary radii. Therefore, when Saturn's magnetosphere is compressed due to high solar wind dynamic pressure, Titan can cross the magnetopause of its parent planet in the subsolar region of its orbit. In such a situation, Titan's ionosphere is exposed to the shocked solar wind plasma inside Saturn's magnetosheath. During the T32 flyby on 13 June 2007, Cassini



Correspondence to: S. Simon  
(sven.simon@tu-bs.de)

became the first spacecraft to provide in-situ observations of Titan's plasma environment while the moon was standing outside the rotating magnetosphere of its parent planet. Titan was located at about 13:45 local time on its orbit around Saturn. At closest approach (17:46:11 UT at an altitude of 975 km above Titan's surface), Titan was located within the shocked magnetosheath plasma. Until several minutes before the encounter, the moon had been exposed to the rotating plasma inside Saturn's magnetosphere. During the flyby, the Cassini magnetometer detected an almost complete reversal of the ambient magnetic field. The density of the impinging plasma also increased dramatically during the pass (Bertucci et al., 2007; Coates et al., 2007; Bertucci et al., 2008). Thus, in the T32 scenario, Titan's upper atmosphere and ionosphere were affected by a sudden change in the properties of the upstream plasma as well as in the direction and magnitude of the ambient magnetic field vector. The purpose of the present study is to analyze these key features of the T32 scenario within the framework of a numerical simulation model.

Following Cassini's arrival in the Saturnian system, a huge number of numerical simulation tools have been applied to support the analysis of plasma and magnetometer data that were collected in the vicinity of Titan. Within the framework of a single-fluid, multi-species Hall-MHD approach, Ma et al. (2006) succeeded in reproducing the key features of Cassini magnetic field measurements during the first two Titan encounters in 2004. Subsequently, this model has been successfully applied to the Cassini T9 encounter (Ma et al., 2007), which has so far been the only opportunity to study the properties of Titan's induced magnetotail at a relatively large distance of about  $4 R_T$  (radius of Titan:  $R_T=2575$  km) to the moon. Another application of the MHD approach to Titan's plasma interaction has been presented by Neubauer and Backes (Backes et al., 2005; Backes, 2005; Neubauer et al., 2006) who also accomplished a reproduction of magnetic field observations during the first series of Titan flybys. The MHD codes are able to reproduce complex ionospheric chemistry in a self-consistent manner, and they also permit a formidable grid resolution of less than 50 km in the immediate vicinity of Titan. However, these models cannot reproduce any kind of velocity difference between different ion components. This constraint is overcome by multi-fluid models. Recently, the first multi-fluid description of Titan's plasma interaction has been presented by Snowden et al. (2007). However, even this approach is unable to reproduce non-Maxwellian distribution functions, such as the ring distributions that are characteristic for pick-up processes. In the Titan scenario, these effects may become important, as the characteristic length scales of the interaction region are comparable to the gyroradii of the involved ion species (Luhmann, 1996; Simon et al., 2007b). The influence of finite ion gyroradii is covered by the semi-kinetic or hybrid models, which apply a fluid description to the electrons of the plasma, whereas the ions are represented by individual par-

ticles. Currently, at least four hybrid models of the Titan interaction are available: Although the first approach developed by Brecht et al. (2000) neglected the finite ion temperature of the impinging magnetospheric plasma, it allowed to obtain valuable information on the orientation of Titan's plasma wake with respect to the corotational flow direction. The hybrid model presented by Kallio et al. (2004) was the first one to cover the real subsonic nature of the magnetospheric plasma in the vicinity of Titan. The codes developed by Modolo and co-workers (Modolo et al., 2007; Modolo and Chanteur, 2008) as well as Simon and co-workers (cf. Simon et al., 2008b and references therein) did not only consider the multi-component nature of the magnetospheric and ionospheric plasmas, but these authors also accomplished successful reproductions of Cassini data collected during recent flybys. A more detailed comparison of the available models is given by Simon et al. (2008a).

Within the framework of the present study, we have applied our multi-species, three-dimensional hybrid model to the situation during the T32 flyby of Titan, i.e. we have tried to investigate the influence of sudden changes in the upstream plasma parameters on the structure of Titan's induced magnetosphere. The results presented here directly succeed the first published attempt to model ion pick-up at Titan in a non-stationary electromagnetic environment (Simon et al., 2008a). Despite having been carried out in the months before the T32 encounter, this preceding study also contains a first analysis of the influence of a magnetopause crossing on the structure of Titan's plasma wake. Before this study, time-dependent models were available only for the plasma interaction of Jupiter's moon Io (Saur and Strobel, 2004). The present paper is organized as follows: In Sect. 2, we give a brief overview of the characteristics of the simulation model. We also discuss the input parameters used for the simulations. Since the technique for modeling non-stationary upstream conditions is the same as in the preceding study, we focus on the major changes that had to be included into the simulation code. In Sect. 3, we discuss in detail our real-time simulation results for the T32 magnetopause crossing. Finally, Sect. 4 provides a summary of our major findings and discusses the limits of applicability to the real situation during T32.

## 2 Model description and simulation parameters

The hybrid approach treats the electrons of the plasma as a massless, charge-neutralizing fluid, while the ions are represented by macroparticles. Therefore, a hybrid model is able to fully resolve effects that are associated with the finite ion gyroradius, such as velocity differences between different plasma constituents or non-Maxwellian distribution functions. The key features of our hybrid simulation model are discussed in detail in our preceding publications: Simon et al. (2006b) and Simon (2007) discuss the basic equations of this

simulation approach as well as the ionosphere model applied to Titan. The initial model considered only one magnetospheric and one ionospheric ion species. An extension of this original model to the case of multi-species upstream and ionosphere conditions has been discussed in detail by Simon et al. (2007b). Recently, this model has been employed to conduct the first numerical investigation of ion pick-up processes at Titan under non-stationary upstream plasma conditions (Simon et al., 2008a). This study did not only consider periodic oscillations of the upstream plasma parameters, but a first attempt to model the influence of a magnetic field reversal at the magnetopause has been presented as well. The results of this preceding study will therefore provide a reference for the interpretation of the T32 simulations presented in this paper. The hybrid model used for this study has also been successfully applied to quantitatively reproduce the magnetic field measurements during the Cassini T9 and T34 flybys of Titan (Simon et al., 2007c, 2008b). Applications of our hybrid model to the plasma interactions of Mars (Böswetter et al., 2004; Simon et al., 2007a; Böswetter et al., 2007), of magnetized asteroids (Simon et al., 2006a) and comets (Bagdonat and Motschmann, 2002a,b; Bagdonat, 2005; Motschmann and Kührt, 2006) have also been published in recent years.

Therefore, only a brief overview of the basic equations of our model shall be given, accompanied by a discussion of the simulation parameters used for the present study. The basic equations of the hybrid model read as follows:

- Equations of motion for individual ions:

$$\frac{d\mathbf{x}_s}{dt} = \mathbf{v}_s \quad \text{and} \quad \frac{d\mathbf{v}_s}{dt} = \frac{q_s}{m_s} \{ \mathbf{E} + \mathbf{v}_s \times \mathbf{B} \}, \quad (1)$$

where  $\mathbf{x}_s$  and  $\mathbf{v}_s$  denote the position and the velocity of an ion of species  $s$ , respectively. The vectors  $\mathbf{E}$  and  $\mathbf{B}$  are the electromagnetic fields. The ion mass and charge are denoted by  $m_s$  and  $q_s$ , respectively.

- Electric field equation:

$$\mathbf{E} = -\mathbf{u}_i \times \mathbf{B} + \frac{(\nabla \times \mathbf{B}) \times \mathbf{B}}{\mu_0 e n_e} - \frac{\nabla P_{e,1} + \nabla P_{e,2}}{e n_e} \quad (2)$$

where  $\mathbf{u}_i$  is the mean ion velocity. The plasma is quasi-neutral, i.e. the mean ion ( $n_i$ ) and electron density ( $n_e$ ) are assumed to be equal. As in general, the electron temperature in a planetary ionosphere differs significantly from the electron temperature in the ambient plasma flow, two different electron pressure terms  $P_{e,1}$  and  $P_{e,2}$  have been incorporated into the simulation model. Specifically, a two-species/single-fluid description is applied to the electrons, i.e. the model discriminates between the densities of the two electron populations, but both of them are assigned the same velocity. In our Titan simulations, the first pressure

term refers to the ambient magnetospheric (or magnetosheath) flow, while the second one represents Titan's ionospheric electrons. Details are discussed in our companion papers (cf. especially Eqs. 4–9 in Simon et al., 2006b, and Eqs. 2–8 in Simon et al., 2007b). Both electron populations are described by adiabatic laws:

$$P_{e,1} \propto \beta_{e,1} n_{e,1}^\kappa \quad \text{and} \quad P_{e,2} \propto \beta_{e,2} n_{e,2}^\kappa, \quad (3)$$

where  $\beta$  are the plasma betas and  $\kappa$  is the adiabatic exponent. For the simulations presented in this work, a value of  $\kappa=2$  has been chosen (Böswetter et al., 2004; Simon et al., 2006a,b).

- Magnetic field equation: By using Faraday's law, an expression describing the time evolution of the magnetic field can be obtained:

$$\frac{\partial \mathbf{B}}{\partial t} = \nabla \times (\mathbf{u}_i \times \mathbf{B}) - \nabla \times \left[ \frac{(\nabla \times \mathbf{B}) \times \mathbf{B}}{\mu_0 e n_e} \right]. \quad (4)$$

Because of the adiabatic description of the electrons, the electron pressure terms do not appear in this equation (Simon et al., 2007a, 2008a).

We have considered two simulation scenarios, both of them basically working as follows: in a first step, the simulation is allowed to achieve a quasi-stationary state. The upstream parameters that have been employed in this first step correspond to the situation inside the magnetosphere of Saturn. After the stationary state has been achieved, the upstream plasma parameters and the magnetic field at the left-hand boundary of the cubic simulation domain (cf. Fig. 1) are suddenly changed, representing Titan's passage through the magnetopause. Then, the simulation is allowed to achieve the quasi-stationary state again, with Titan now being embedded into the magnetosheath plasma flow. This procedure is identical to the method which is discussed in Sects. 2 and 7 of our companion paper (Simon et al., 2008a, cf. the discussion of simulation run #5 in that work).

In both simulation scenarios under consideration, the upstream plasma flow inside Saturn's magnetosphere is assumed to consist of oxygen ( $\text{O}^+$ ) and hydrogen ( $\text{H}^+$ ) ions. Their number densities in the undisturbed plasma were set to  $n(\text{O}^+)=0.2 \text{ cm}^{-3}$  and  $n(\text{H}^+)=0.5n(\text{O}^+)$ , respectively. The temperatures are given by  $kT(\text{O}^+)=2900 \text{ eV}$  and  $kT(\text{H}^+)=210 \text{ eV}$ . These values correspond to the "classical" Voyager 1 scenario of the Titan interaction which has been discussed in detail by Neubauer et al. (1984), and which also provided the input parameters for most of the existing simulation models (see e.g. Ledvina et al., 2004; Simon et al., 2008a). The plasma impinges on Titan's ionosphere with a relative velocity of  $u_0=120 \text{ km/s}$ , the flow being aligned with the positive  $x$ -axis of the coordinate frame shown in Fig. 1. As for the plasma composition in the magnetosheath, two different cases are considered:

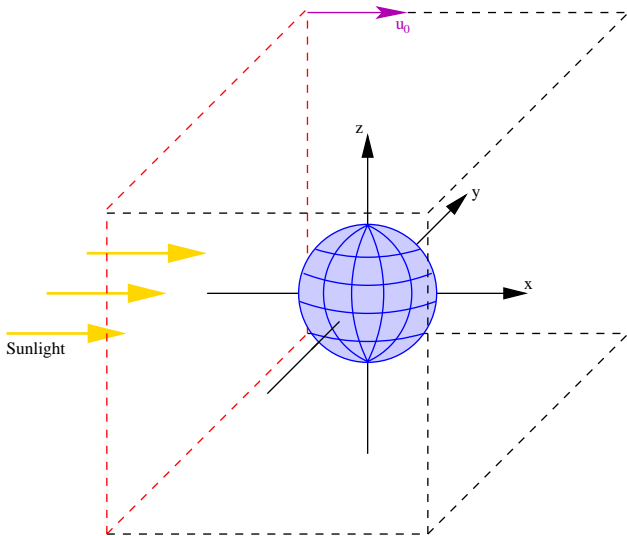


**Fig. 1.** Simulation geometry. The center of Titan coincides with the center of the cubic simulation domain, its extension being  $\pm 7.5 R_T$  in each spatial direction. The upstream plasma direction  $u_0$  as well as the direction of the ionizing solar UV radiation are aligned with the positive  $x$  axis, i.e. Titan's dayside is located in the ( $x < 0$ ) half space of the coordinate frame. Titan's orbital plane coincides with the ( $x, y$ ) plane of the coordinate system. All faces of the simulation box except for the left one (as denoted by the red dashed lines) have been treated as outflow boundaries. At first, the simulation is allowed to achieve a quasi-stationary state, representing the situation inside the magnetosphere. Then, the boundary conditions at the ( $x = -7.5 R_T$ ) face of the simulation domain are instantaneously modified in order to mimic the magnetopause crossing. The modified magnetic field vector is then convected towards Titan by the plasma flow. With these new boundary conditions, the simulation is allowed to achieve a stationary state again, illustrating the structure of Titan's plasma environment in Saturn's magnetosheath.

#### 1. Simulation run # 1:

Like the plasma inside the magnetosphere, the flow in the magnetosheath includes an oxygen component of density  $n(O^+) = 0.2 \text{ cm}^{-3}$ . However, the hydrogen density inside the magnetosheath is about a factor of 13 larger than inside the magnetosphere. The total plasma density is therefore  $n = 1.5 \text{ cm}^{-3}$ . The reader should notice that currently, no definite density values from the Cassini plasma instruments are available.

#### 2. Simulation run # 2:

We have investigated the case of a magnetosheath plasma that consists of light hydrogen ions only, i.e. the heavy oxygen component is absent inside the magnetosheath. The total hydrogen density inside the magnetosheath is given by  $n(H^+) = 3.2 \text{ cm}^{-3}$ . Due to this relatively large value for the proton density, the ram pressure of the impinging magnetosheath plasma is only about 20% smaller than in the first simulation scenario. Thus, the discussion can entirely fo-

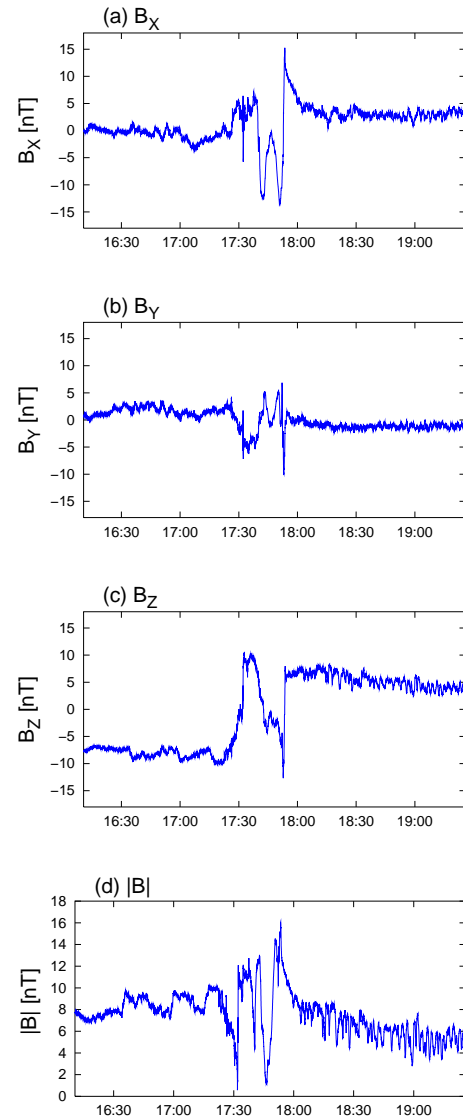


**Fig. 2.** Titan's magnetic field signature during Cassini's T32 flyby with respect to the Titan Interaction System TIIS. Cassini's closest approach took place on 13 June 2007 at 17:46:11 UT. The magnetic field almost reversed its direction during the magnetopause crossing. As can be seen in the inbound region of the flyby, the magnetic field inside the magnetosphere was pointing "downward" with respect to Titan's orbital plane, i.e.  $B_Z < 0$ . In the outbound region of the flyby, the magnetic field was directed "upward", i.e.  $B_Z > 0$ . The magnetic field data were first published and discussed by Bertucci et al. (2008).

cus on the question of how the magnetic reconfiguration process is affected by different particle masses in the upstream magnetosheath flow. If a hydrogen density of  $n(H^+) = 1.5 \text{ cm}^{-3} = n(e^-)$  was assumed for Saturn's magnetosheath, the difference to the magnetosheath ram pressure in run # 1 would be significantly larger. Besides, when using a value of  $n(H^+) = 3.2 \text{ cm}^{-3}$

**Table 1.** Mach numbers for T32 simulations:  $M_A$  (alfvénic),  $M_S$  (sonic) and  $M_{MS}$  (magnetosonic). In run # 1, the magnetosheath plasma consists of hydrogen as well as oxygen. In run # 2, the magnetosheath plasma does not include an oxygen component.

Plasma regime	$n(\text{O}^+) [\text{cm}^{-3}]$	$n(\text{H}^+) [\text{cm}^{-3}]$	$M_A$	$M_S$	$M_{MS}$
Magnetospheric plasma (runs # 1 and # 2)	0.2	0.1	1.15	0.82	0.67
Magnetosheath plasma (run # 1)	0.2	1.3	1.88	0.82	0.75
Magnetosheath plasma (run # 2)	0	3.2	1.66	0.82	0.73

for the sheath plasma, the discontinuity represents a surface of perfect pressure balance between magnetospheric and magnetosheath plasma regime, i.e. the sum of ram pressure, thermal pressure and magnetic pressure is the same on both sides.

The magnetic field magnitude and orientation have been chosen in agreement with Cassini magnetometer measurements. The time series of the Cassini MAG instrument (Dougherty et al., 2004) for the T32 flyby in TIS coordinates (Backes, 2005; Backes et al., 2005) is displayed in Fig. 2. In the inbound region of T32, the magnetic field was directed “downward” with respect to Titan’s orbital plane, i.e.  $B_Z < 0$ . In contrast to this, the magnetosheath field was directed “upward”, i.e.  $B_Z > 0$ . The upstream magnetic field values for the simulations have been chosen in such way that they can be considered reasonable approximations to the nearly homogeneous segments in the inbound and outbound regions of the measured T32 field signature. In both simulations, the magnetic field vector inside the magnetosphere is given by  $\mathbf{B} = (0, 1.5, -8)$  nT with respect to the coordinate frame shown in Fig. 1. After the simulation has achieved its quasi-stationary state, the magnetic field vector in the left-hand boundary of the simulation box is suddenly changed to  $\mathbf{B} = (0, -1.2, 5.8)$  nT. The modified magnetic field is then “frozen into” the newly generated plasma at the left-hand inflow boundary and is subsequently convected towards Titan by the impinging plasma flow (see also Sect. 2 of Simon et al., 2008a). Now including the modified field direction, the simulation scenario achieves a quasi-stationary state again. This final state illustrates the structure of Titan’s plasma environment when the moon is located outside the rotating plasma of Saturn’s magnetosphere. Given the parameters discussed above, the plasma flow inside the magnetosphere as well as in Saturn’s magnetosheath is super-alfvénic, yet subsonic and submagnetosonic. The specific Mach numbers are listed in Table 1.

The simulation approach described above is able to cover some basic features of Titan’s plasma interaction during the Cassini T32 flyby. However, the reader should also be aware that the model includes the following limitations and simplifying assumptions: The model does not consider a change of the plasma velocity across the magnetopause boundary. Neither the flow direction nor the magnitude of  $u_0$  is altered in our representation of the magnetopause crossing. Due to the

numerical difficulties that are associated with the implementation of outer boundary conditions in Titan simulations (cf. Kallio et al., 2004, or Simon, 2007, for a detailed discussion), this constraint may not be overcome by any semi-kinetic simulation code. In the simulation scenario presented here, the impinging plasma flow is always directed in (+x) direction, the flow velocity being  $u_0 = 120$  km/s. The discontinuity is travelling into the simulation box with exactly the same velocity, i.e. it is synchronously transported by the plasma flow. The flow velocity and direction in Saturn’s magnetosheath during T32 are still unknown. Thus, despite not being capable of quantitatively reproducing all observed features, the systematic approach chosen in this paper might at least provide an impression of several basic effects that occur when Titan’s plasma environment is exposed to sudden changes of the upstream conditions. Although it is not possible to change the upstream flow velocity and direction while the simulation proceeds, it is of course easy to conduct a simulation that includes e.g. a reduced flow velocity from the beginning. Such simulations of the Titan interaction (i.e. a sub-alfvénic, subsonic and submagnetosonic scenario) have been presented in the companion paper by Simon et al. (2006b). These results will provide a qualitative reference for the discussion below.

Besides, the simulations presented here do not consider a difference between the temperatures of the upstream constituents on both sides of the boundary layer. However, we have conducted careful tests, using a reduced upstream plasma temperature inside the magnetosheath. We have even conducted a (hypothetical) test run in which the magnetosheath plasma was assumed to be so cold that a shock wave was formed ahead of Titan. These simulations have shown that the temperature of the impinging magnetosheath plasma does *not* play a decisive role for the characteristic time scales of the magnetic field reconfiguration process. Therefore, we have decided to keep the scenario as simple as possible and not to include a temperature change at the boundary between both plasma regimes into our final simulations. Due to this simplification, the boundary between both plasma regimes in simulation run # 1 is not a surface of perfect pressure balance between magnetospheric and magnetosheath plasma ( $p_{\text{magnetosphere}} = 0.8 p_{\text{sheath}}$ ). However, as will also be demonstrated below, the model boundary between magnetospheric and magnetosheath plasma regimes has shown to be absolutely stable on the time scales of our simulations. Besides,

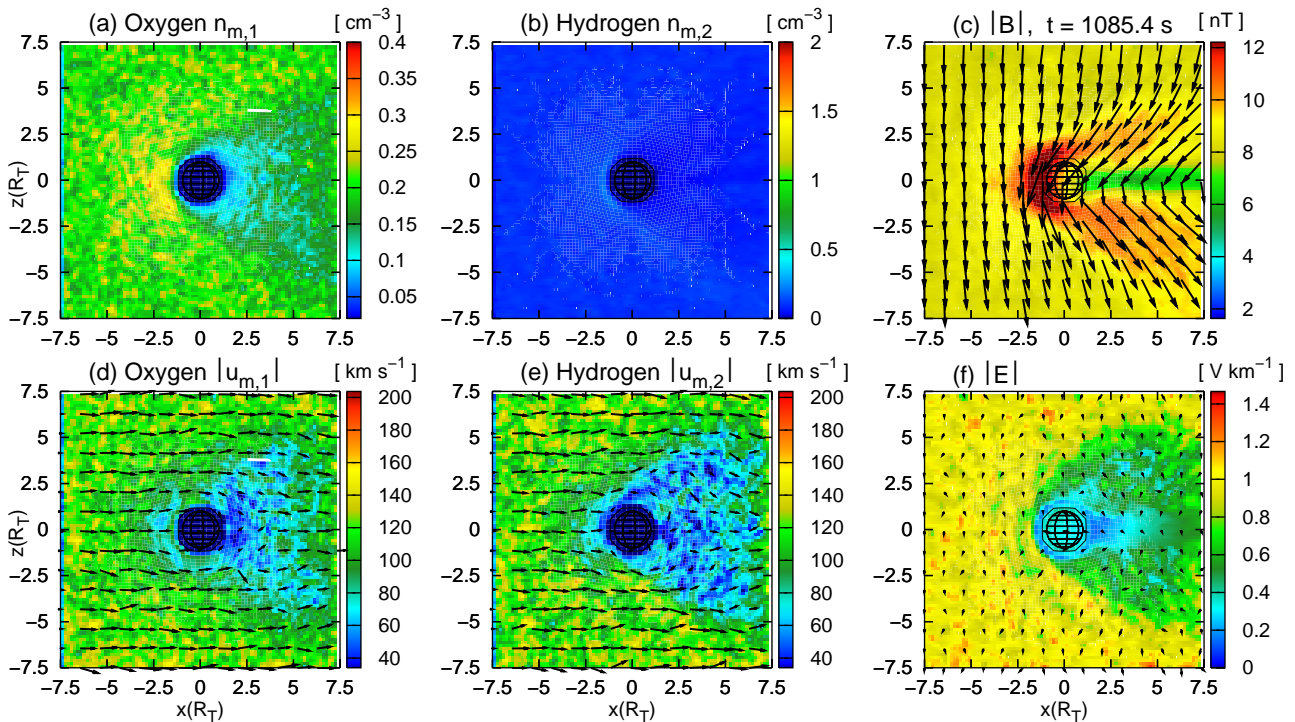


**Fig. 3.** Run # 1. Flip-book of Titan's plasma interaction during Cassini's T32 flyby. The figure illustrates the quasi-stationary state of the simulation that is achieved *before* the magnetopause discontinuity enters the simulation domain from the left-hand side. For a cut through the  $(x, z)$  plane of the coordinate frame, the figure displays (a) the oxygen number density  $n_{m,1}$ , (b) the hydrogen number density  $n_{m,2}$ , (c) the magnetic field magnitude and direction, (d) the oxygen velocity  $u_{m,1}$ , (e) the hydrogen velocity  $u_{m,2}$  and (f) the electric field. The nomenclature used in the figure is the same as in our preceding publications. This illustration of the situation inside the magnetosphere is valid for run # 2 as well.

there is no evidence that Saturn's magnetopause was in a state of equilibrium during T32 (Bertucci et al., 2008).

In all simulation runs, Titan's ionosphere is assumed to consist of three species with representative masses: molecular nitrogen ( $N_2^+$ ), methane ( $CH_4^+$ ) and molecular hydrogen ( $H_2^+$ ). Titan's dayside ionosphere is located in the  $(x < 0)$  half space of the coordinate frame (cf. Fig. 1). The dayside ionosphere is represented by a Chapman layer, i.e. the local ion production rate depends on both the altitude above the surface and the solar zenith angle. The model is based on a three-term neutral profile, consisting of two (barometric) exponential terms with different scale heights and a  $1/r$  term to describe the exosphere. Like the "classical" one-term Chapman production function, the dayside ionosphere in the model includes a  $\exp(-1/\cos \chi)$  dependency on the solar zenith angle  $\chi$ . Details are discussed in Sect. 2.2 of Simon et al. (2006b), cf. especially Figs. 2 and 3 as well as Table 1 in that work. The nightside production profile includes a dependency on the altitude, but it is of course independent of the solar zenith angle. The free parameters of the ionosphere model employed for this study are the same as in the companion papers (Simon et al., 2006b, 2007b). An alternative approach, allowing a self-consistent computation

of the ion production rates, has been developed by Modolo and Chanteur (2008). Like our model, this approach has recently been successfully applied to explain some of the observed features during the Cassini T9 flyby of Titan (Modolo et al., 2007). The ion production profile in our model is not computed self-consistently, but the number of ionospheric macroparticles inserted into the box per time unit can be considered to represent the equilibrium state between continuous production due to ionization and continuous removal of ions due to recombination. In other words, these processes are included in a phenomenological way.

Our simulations are carried out on a so-called Fisheye grid, allowing an enhanced spatial resolution near Titan's surface. The grid consists of 90 nodes in each spatial direction. The major advantage of this curvilinear grid is that in Titan's ionosphere, the radial grid resolution can locally be enhanced to a value of about  $0.09 R_T$  (radius of Titan:  $R_T=2575$  km). In the undisturbed magnetospheric flow far away from Titan, the grid smoothly transforms into a Cartesian grid and features a cell resolution of  $0.16 R_T$ . Details are discussed by Simon et al. (2006b), cf. especially plot 4 in that work. As displayed in Fig. 1, the center of Titan coincides with the center of the simulation domain, also defining the origin of the Cartesian reference coordinate frame. The box possesses

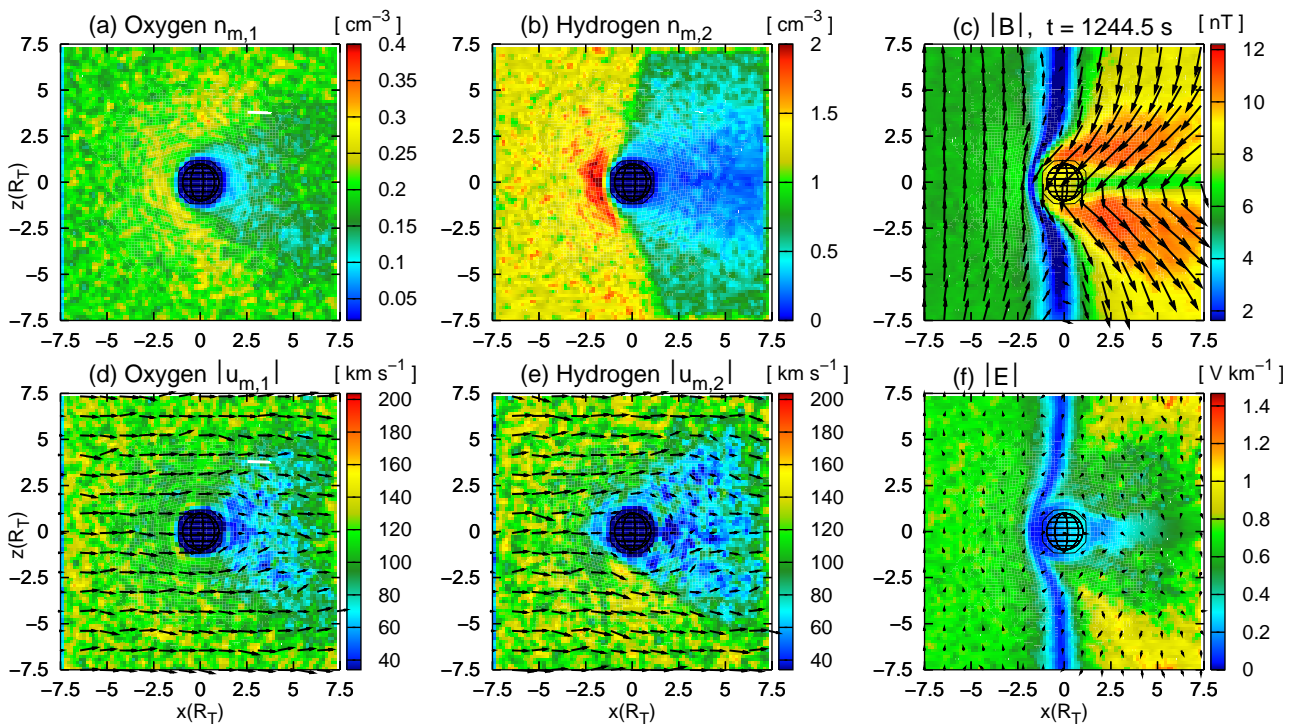


**Fig. 4.** Run # 1. Flip-book of Titan's plasma interaction during Cassini's T32 flyby. The quantities displayed in the figure are the same as in Fig. 3. The thin discontinuity between magnetospheric and magnetopause plasma regime has entered the simulation domain from the left-hand side and has now arrived at Titan's ramside. Note the differences between magnetic field magnitude and direction on both sides of the discontinuity and the resulting effect on the electric field strength. The original magnetic pile-up region at Titan's ramside has already been almost completely eroded due to reconnection. The magnetotail is still unaffected. The draping pattern at Titan's wakeside is compressed with respect to the original configuration (cf. plot (c) in Fig. 3). As can be seen from plot (b), the hydrogen density already starts to increase at Titan's ramside.

a spatial extension of  $\pm 7.5 R_T$  in each spatial direction. Any particle that hits the surface of Titan is removed from the simulation, whereas in the obstacle's interior, no boundary conditions are imposed on the electromagnetic fields. The advantages and disadvantages of this type of inner boundary treatment are discussed by Böswetter et al. (2004) and by Simon et al. (2007a). Initially, each cell of the simulation grid is filled with about 30 magnetospheric macroparticles, whereas in the obstacle's ionosphere, a total number of 1500 new macroparticles is generated during each time step.

### 3 Results of real-time simulations

This section deals with the results of our real-time simulations for T32. Of course, the most instructive way to present the results would be a movie, giving a real-time illustration of the reconfiguration of Titan's plasma tail. In a printed journal, we can only show a sequence of snapshots, i.e. a flip-book that illustrates the key elements of the reconfiguration process. Before commencing our discussion, we would like to point out that each simulation run consists of three basic steps. Each simulation is initiated at  $t=0$ . At this point, the simulation box around Titan is filled with undisturbed

plasma, its composition and velocity corresponding to the situation inside Saturn's magnetosphere. The quasi-stationary state that is computed from this initial configuration illustrates the signatures in Titan's plasma environment while the moon is located inside the rotating magnetosphere of its parent planet. The quasi-stationary state of the simulation is achieved after a duration in which the undisturbed magnetospheric plasma would have passed three times through the entire simulation domain of length  $15 R_T$ , i.e. after about 966 s. About two minutes after this quasi-stationary state has been achieved, the plasma and magnetic field parameters at the left-hand face of the simulation box are reconfigured, now representing the anticipated characteristics of the upstream flow in Saturn's magnetosheath. The discontinuity between both regimes is then convected towards Titan by the newly generated plasma flow. After the modified upstream plasma has fully embedded Titan, the simulation proceeds towards a quasi-stationary state, which is again achieved after 2–3 passages of the flow through the simulation domain. In the following, we present snapshots of both quasi-stationary states as well as the (non-stationary) magnetic reconfiguration process that is initiated when the discontinuity arrives at Titan's ramside ionosphere.

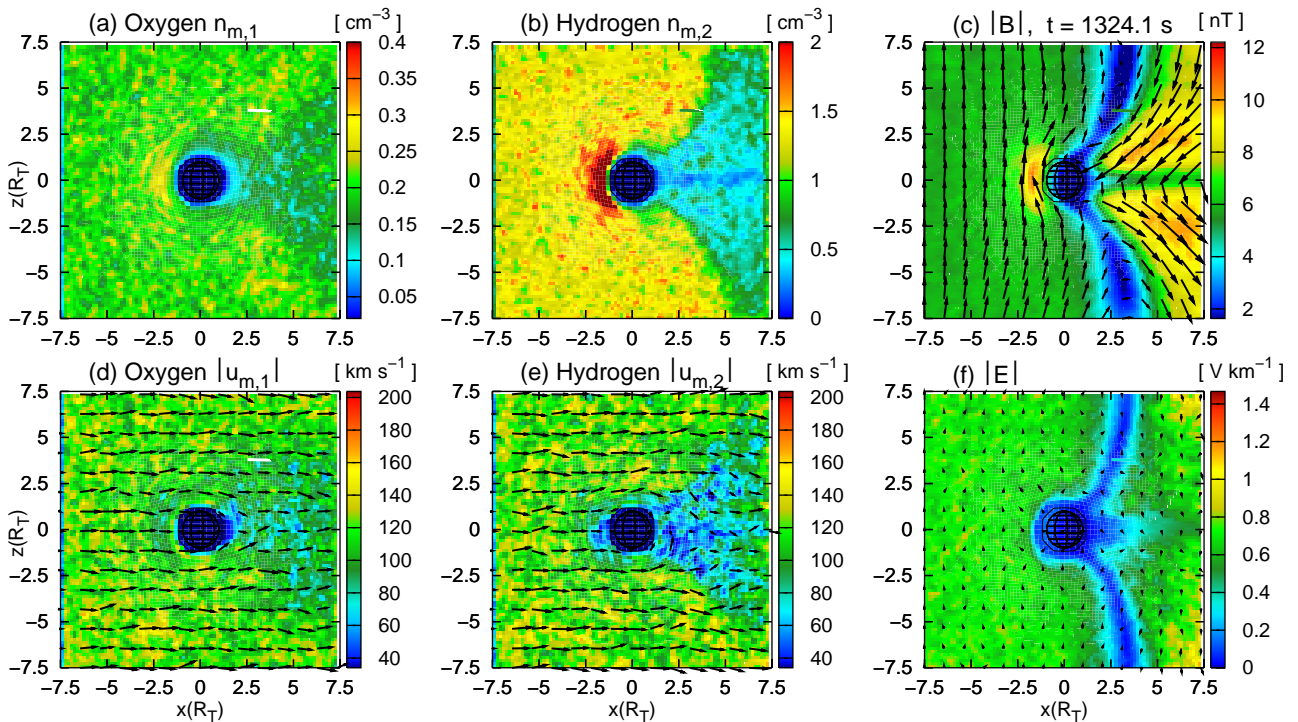


**Fig. 5.** Run # 1. Flip-book of Titan's plasma interaction during Cassini's T32 flyby. The quantities displayed in the figure are the same as in Fig. 3. After the magnetic pile-up region at Titan's ramside has been completely eroded, the magnetosheath field now starts to drape around the moon's ionosphere and the ramside magnetic barrier is rebuilt. At Titan's wakeside, the magnetotail is reconfigured due to reconnection. Note especially the newly merged field lines upwards and downwards of Titan (in the "blue" arms of the discontinuity) which are no longer in contact with the moon's ionosphere.

### 3.1 Run # 1: Oxygen and hydrogen in the magnetosheath

As discussed above, in our first simulation run, the magnetosheath plasma consists of both oxygen and hydrogen ions, the total number density matching the value obtained from the Cassini electron spectrometer. Figures 3 to 7 provide a series of snapshots, illustrating the simulation results. The plots show two-dimensional cuts through the  $(x, z)$  plane of the coordinate frame which contains the upstream flow vector as well as the major component of the magnetic field. Figure 3 displays the first quasi-stationary state of the simulation, i.e. the plasma environment of Titan when the moon is located inside the rotating magnetosphere of Saturn. Figures 4 to 6 illustrate how the magnetopause discontinuity travels through the simulation domain. The final state of the simulation, showing Titan's plasma environment when being located within the magnetosheath of Saturn, can be seen in Fig. 7.

When Titan is located inside Saturn's magnetosphere, the structure of the moon's plasma tail features a strong qualitative resemblance to the scenarios that have been discussed in our companion publications. Therefore, only the key features shall be briefly pointed out. It should be noted that the

color scale in the hydrogen density plot 3b has been chosen to resolve the signatures that will be visible after the magnetosheath entry. Therefore, the deflection pattern that arises in the  $H^+$  density inside the magnetosphere is not visible here. The hydrogen flow pattern for the case of Titan being located inside Saturn's magnetosphere is analyzed in detail in our companion study (Simon et al., 2007b). As can be seen from Fig. 3c, the Saturnian magnetic field lines form a pronounced draping pattern in the vicinity of Titan. In the pile-up region adjacent to Titan's ramside ionosphere, the background magnetic field strength is exceeded by more than a factor of 1.5. As can be seen from the velocity plots 3d and 3e, a cone-like deflection region of reduced magnetospheric plasma velocity arises downstream of Titan.

Figures 4, 5 and 6 illustrate the passage of the discontinuity through the interaction region. As can be seen e.g. from plots 4b and 4c, the hydrogen density at the left-hand side of the discontinuity is increased, while the magnetic field direction is reversed with respect to the orientation in the downstream region. The field magnitude in the magnetosheath plasma is also smaller than inside the magnetosphere. As displayed in Fig. 4c, when the magnetosheath magnetic field meets the pile-up region at Titan's ramside ionosphere, the original pile-up region is eroded due

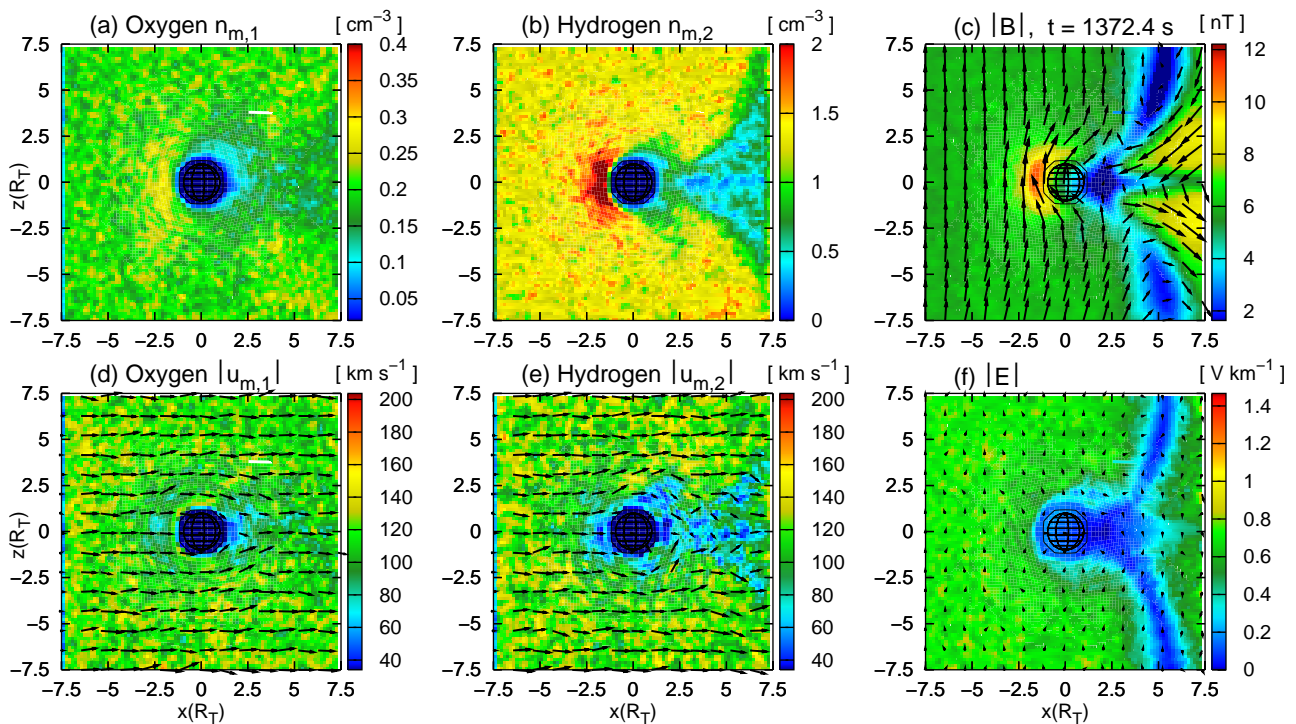


**Fig. 6.** Run # 1. Flip-book of Titan's plasma interaction during Cassini's T32 flyby. The quantities displayed in the figure are the same as in Fig. 3. The figure shows another snapshot of the magnetic reconfiguration process. The field strength at Titan's ramside has almost achieved its final value. Note that only about two minutes have passed since the erosion of the original magnetic pile-up region had been completed. The field strength achieved in the remaining fragments of the wakeside magnetic lobes is about 4 nT smaller than the value obtained from Figs. 3 and 4. The reason for this is that these field lines are no longer strongly draped around Titan, but they lead to the reconnection region along the discontinuity. Therefore, the magnetic pressure in the lobe regions has already been reduced. Plot (b) illustrates how the Titan wake is filled by the increased hydrogen density in Saturn's magnetosheath. Due to the high thermal velocity, the region dominated by the newly added hydrogen population does not feature a sharp, but rather a diffuse outer boundary. This can be seen quite well along the outer flanks of the cone-like wake structure in plots (b) and (e).

to magnetic reconnection. The newly merged field lines can be seen quite well around the  $x = -1.5 R_T$  line in plot 4c, above and below Titan. When the discontinuity arrives at Titan, the wakeside magnetic lobes are initially compressed for a short time, which is why the peak field strength achieved in the wakeside draping pattern at  $t = 1244.5$  s is slightly larger than in the original quasi-stationary state, cf. plot 3c. After the original ramside pile-up region has been completely eroded by the reconnection process, the discontinuity is able to pass the ramside ionosphere of Titan and the reconfiguration process in the wakeside magnetic lobes commences. As can be seen in plot 5c, there is a certain retardation between the travelling of the discontinuity through the ionosphere of the obstacle and its motion along the outer flanks of the interaction region. The deformation of the discontinuity due to this "sticking effect" in the immediate vicinity of Titan is also well illustrated in Fig. 6c. As shown in the sequence of magnetic field plots 3c to 6c, after the original pile-up region has been removed, the magnetosheath field immediately starts to drape around the moon's ramside ionosphere and the pile-up region is rebuilt. Thus, the magnetic field configuration

shown in Fig. 6c contains four different regions: When moving from negative to positive  $x$  values, at first, the magnetosheath region with its undisturbed, reversed magnetic field vector is passed. In the vicinity of Titan – but still upstream of the discontinuity – the newly forming magnetic pile-up region above the ramside ionosphere is encountered. This region is followed by the discontinuity itself, along which the magnetic reconfiguration process takes place. Finally, in the downstream region, the remnants of the original magnetic lobe structure can be found.

At the wakeside of Titan, contact between the original magnetospheric draping pattern and the oppositely directed magnetic field lines upstream of the discontinuity leads to magnetic reconnection again. Overall, this process yields a reversal of the magnetic field polarity in the wakeside lobes of Titan. The removal of the original lobe structure due to the reconnection process is well illustrated in plots 5c and 6c. Near the discontinuity, newly merged magnetic field lines which are not in contact with Titan any more are formed in the ( $z > 1 R_T$ ) as well as in the ( $z < 1 R_T$ ) half space. This process also leads to a relaxation of the wakeside magnetic

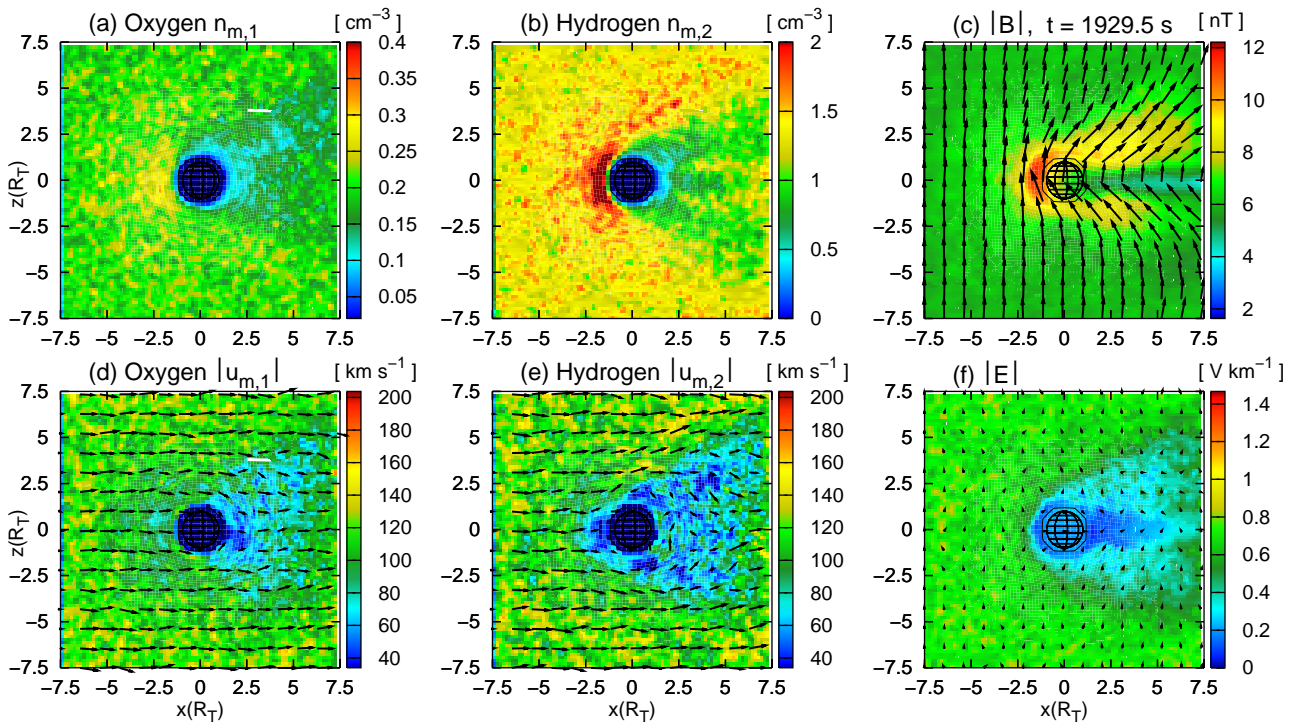


**Fig. 7.** Run # 1. Flip-book of Titan's plasma interaction during Cassini's T32 flyby. The quantities displayed in the figure are the same as in Fig. 3. The figure illustrates the final state of the simulation, with Titan now being embedded into the dense plasma of Saturn's magnetosheath. The polarity of the magnetotail has completely reversed. A cone-like wake cavity is visible in the hydrogen density, as shown in plot (b).

lobe structure which had initially been compressed when the discontinuity came into contact with Titan's ramside ionosphere. As can be seen from plot 5c, the peak magnetic field values in the remaining lobe fragments are about 3–4 nT smaller than in the original configuration (cf. Fig. 3c) or before the initiation of the wakeside reconnection process (cf. Fig. 4c). Some time after the discontinuity has left the simulation domain, the situation achieves a quasi-stationary state again, now illustrating the topology of Titan's magnetic environment when the moon is located inside Saturn's magnetosheath. This situation is shown in Fig. 7. As can be seen from plot (c), the magnetic field polarity in the lobes is now reversed. In contrast to the situation inside the magnetosphere where  $B_z$  dominates, the  $B_y$  component of the ambient magnetic field is no longer negligible with respect to the  $B_z$  component. This yields an asymmetry of the newly formed draping pattern with respect to Titan's orbital plane (which is defined by the  $x$ - and  $y$ -axes), as it is illustrated in plot 7c as well. The origin of the asymmetries in Titan's magnetic environment is discussed in detail by Simon et al. (2007b).

The real-time simulation scenario presented here allows to determine the characteristic time scales of the magnetic reconfiguration process. Therefore, each of the simulation plots discussed above contains a time marker, referring to the initiation of the simulation with Titan being embedded

into a homogeneous, featureless magnetospheric plasma flow ( $t=0$ ). The simulations show that the magnetic reconfiguration process needs to be described by two time scales, the first of them characterizing the erosion and rebuilding of the ramside magnetic pile-up region, while the second one refers to the reversal of the magnetic field polarity in the wakeside lobes. Our simulations show that the complete erosion of the original magnetic pile-up region at Titan's ramside (i.e. a decrease from  $B=B_{\max}$  to  $B=0$ , thus achieving a complete demagnetization of the moon's ramside ionosphere) requires a total duration of only about 2–3 min. The build-up of the new ramside pile-up region after the discontinuity has left the ( $x < 1R_T$ ) half space of the coordinate frame requires another 2 min, whereas the newly formed induced magnetotail achieves its quasi-stationary state about 3–4 min after the discontinuity has entered the wakeside half space of our coordinate frame. What should be noted at this point is that the reconfiguration of the overall magnetic field topology in the vicinity of Titan takes place on a characteristic time scale of only a few minutes, and that the simulations show only a minor retardation between the motion of the discontinuity through the interaction region and the re-orientation of Titan's induced magnetotail structure. In other words, the travelling time of the discontinuity through the near-Titan region seems to determine at least a rough measure for the characteristic time of the magnetic reconfiguration process.

The complete remagnetization of Titan's ionosphere (i.e. re-achieving the quasi-stationary state of the simulation) is characterized by only a minor retardation with respect to the travelling of the discontinuity through Titan's wake.

In the following, we shall focus on the behaviour of the ambient plasma parameters during the magnetosheath excursion, as displayed in plots (a), (b), (d) and (e) of the "flip-book". As can be seen in the sequence of plots (d) and (e), the discontinuity included into our simulation model does not manifest in the velocity pattern of the impinging plasma species. This simplification must be considered a major constraint of the simulation approach presented here, since we have demonstrated above that the convection time of the re-oriented magnetic field through the interaction region defines a measure of the characteristic time that is required to achieve stationarity again. However, altering the plasma flow velocity or direction while the simulation proceeds is in principle impossible for any kind of semi-kinetic simulation approach, without the boundary conditions imposed on the outer faces of the simulation domain giving rise to numerical artifacts that may falsify the simulation results (cf. Simon, 2007, for details). Besides, there are no measured flow directions and magnitudes available for the plasma in Saturn's magnetosheath during T32. However, at the present state of research we can try to estimate the influence of different plasma flow velocities and directions in magnetopause and magnetosheath. First of all, in the companion study by Simon et al. (2006b), it has been analyzed how the signatures in Titan's plasma environment are affected when the moon is exposed to a very slow (sub-alfvénic, subsonic and submagnetosonic) magnetospheric flow. It has been demonstrated that reducing the Mach numbers of the upstream flow yields a less compact magnetic pile-up region at Titan's ramside. Besides, the more dominant tension and pressure terms in the magnetic field equation lead to a widening of the magnetic draping pattern, i.e. the opening angle of the Alfvén wing (Neubauer et al., 2006) is increased (see also Sect. 5 of Simon, 2007, for a more extensive discussion). Based on these simulation results, we expect that reducing the upstream flow velocity at the magnetopause would go along with an increase of the reconfiguration time for the magnetotail topology, the time scale again being roughly determined by the now reduced velocity of the upstream flow. A more critical aspect is the fact that the plasma velocity inside the magnetosheath does not have to be aligned with the direction of the rotating plasma flow inside Saturn's magnetosphere. If the orientation of the impinging flow vector changes during a magnetosheath excursion – i.e. if in the "worst case", ramside and wakeside hemisphere of Titan are exchanged –, the originally piled up magnetic field lines may remain for much longer times than inferred from the simplifying approach presented here. However, quantifying these effects is far beyond the scope of the present study, especially since there are no data available to validate the results.

The motion of the magnetosheath plasma flow towards Titan can well be seen in the hydrogen density plot series (b) of Figs. 3 to 7. As can be seen e.g. from Fig. 4b, the hydrogen density clearly increases at Titan's ramside, while the oxygen density pattern is only insignificantly affected. In general, the modification of the magnetospheric flow pattern in the vicinity of Titan is rather weak, due to the thermal velocity of the impinging flow clearly exceeding its bulk speed. For this reason, the Titan interaction does not give rise to a sharply pronounced wake cavity or an Ion Composition Boundary, as they are found in the plasma environments of Venus, Mars or comets (cf. Bößwetter et al., 2004, and references therein).

### 3.2 Run # 1: Tail detachment during the T32 magnetopause crossing?

In this section, we shall focus on the question of how Titan's exospheric ion tail is affected by the moon's passage through the discontinuity. It is known that in the case of comets, crossing of magnetic sector boundaries in the solar wind can yield a detachment of the plasma tail from the nucleus. Within the framework of hybrid simulations, this has been discussed e.g. by Bagdonat (2005). For the Titan scenario, a first study of the influence of tangential discontinuities is also already available (Simon et al., 2008a). In this study, the "classical" Voyager 1 configuration of the Titan interaction had been considered, with the magnetic field inside the magnetosphere being given by  $\mathbf{B} = (0, 0, -5)$  nT in TIS coordinates (see also Neubauer et al., 1984, for details). The magnetopause crossing had been mimicked by simply reversing the magnetic field direction from "downward" to "upward". This original model considered neither a change in the magnetic field magnitude nor in the plasma composition at the boundary layer. The model results had shown that in such a configuration, Titan's exospheric tail is re-oriented, but it is *not* detached from the moon when encountering the tangential discontinuity.

The model presented here is more sophisticated, since the change in the magnetic field magnitude, and therefore in the magnitude of the convective pick-up electric field, is taken into consideration. As can be seen from the (f) sequence of plots in the flip-book, the electric field value upstream of the discontinuity is clearly exceeded by the downstream value. For this situation, the exospheric tail configurations are shown in Figs. 8 and 9. The first plot shows the stationary tail structure when Titan is located inside the magnetosphere, whereas the second one illustrates the situation in Saturn's magnetosheath. The subscript 1 refers to the ionospheric molecular nitrogen component, while the subscripts 2 and 3 denote methane and molecular hydrogen, respectively. The plasma densities (on a logarithmic scale) are shown in the first row, while the plots in the second row display the corresponding mean velocities.

Figure 8 illustrates the structure of Titan's exospheric tail when the moon is located inside the magnetosphere of its

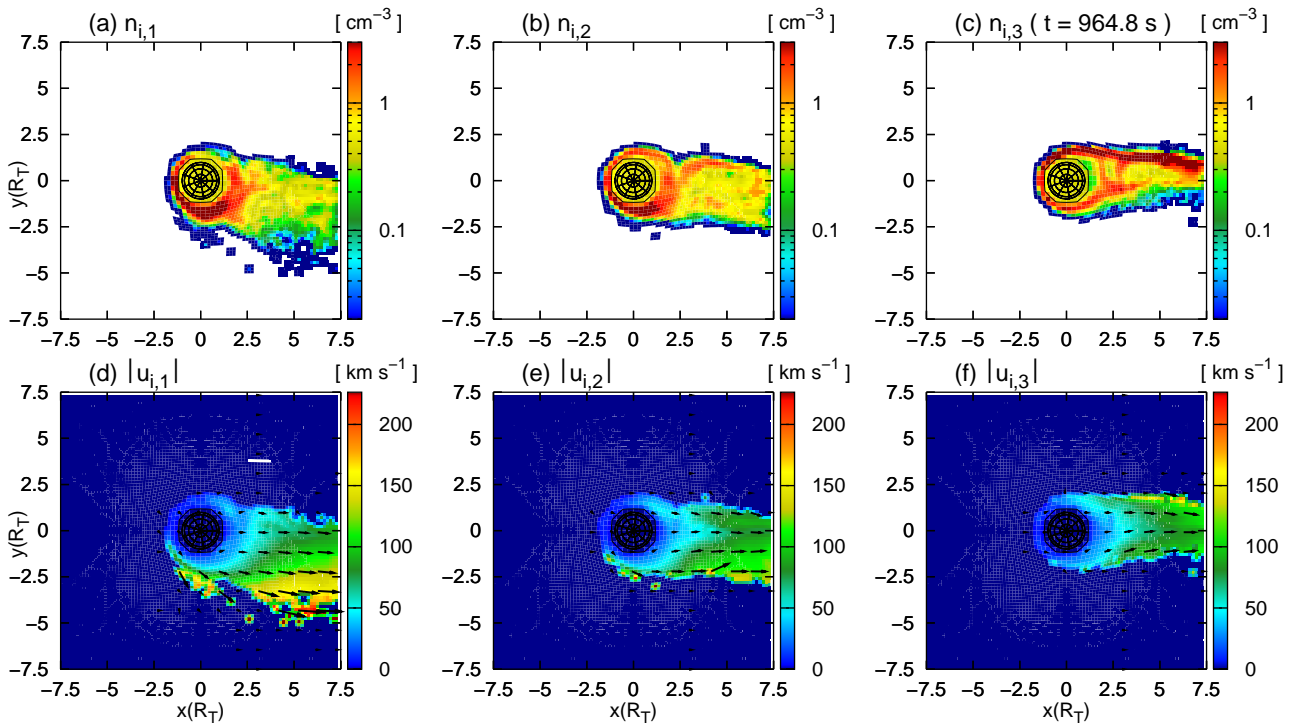


**Fig. 8.** Run # 1. Structure of Titan's ionospheric tail when the moon is located inside Saturn's magnetosphere. For a cut through Titan's orbital plane ( $z=0$ ), the figure displays the densities  $n$  and velocities  $u$  of the three ionospheric species included in the model: molecular Nitrogen  $N_2^+$  (subscript 1, plots **a** and **d**), methane  $CH_4^+$  (subscript 2, plots **b** and **e**) and molecular hydrogen  $H_2^+$  (subscript 3, plots **c** and **f**). In this plane, the particles are moving on cycloidal trajectories, with the spatial extensions of the cycloidal arcs depending linearly on the mass of the pick-up ions.

parent planet. Note that Figs. 8 and 9 show the situation in Titan's *orbital* plane ( $z=0$ ) which is nearly perpendicular to the undisturbed upstream magnetic field vector. Therefore, it contains the cycloidal trajectories of the newly generated pick-up ions. Despite the non-ideality in the magnetic field orientation, numerous features which we have identified in the Voyager 1 configuration (cf. Simon et al., 2008a, and references therein) can be found here as well. For instance, plots 8a to c show the spatial dispersion of ions of different masses in the tail (mass spectrometer effect, see also Luhmann, 1996), although not being as pronounced as in the idealized Voyager 1 scenario. As can be seen from the velocity patterns, at the tail's flank in the ( $y < 0$ ) hemisphere, the peak velocity achieved by the *heaviest* ion species clearly *exceeds* (!) the velocities of the two lighter ionospheric constituents. This effect had been ascribed to the finite gyroradius of the ions and to the interconnection between different pick-up species which is communicated by the electric field.

The crucial result is that, despite the more realistic simulation geometry, Titan's exospheric tail is *not* detached from the satellite during the magnetopause passage. The tail is reconfigured, in the orbital plane now being shifted into the ( $y > 0$ ) hemisphere. This can be seen in Fig. 8, displaying the final, quasi-stationary state of the simulation under mag-

netosheath upstream conditions. However, the reader should again keep in mind the constraint that the model does not include a change of the flow direction across the discontinuity. As for the overall structure of the ionospheric tail, the cut through Titan's orbital plane shown in Fig. 8 illustrates quite well the influence of finite gyroradius effects. Among the three ionospheric species included into the simulation, the molecular nitrogen ions possess the largest gyroradius. Inside the Saturnian magnetosphere, the  $N_2^+$  ions are completely confined to the ( $y < 0$ ) half plane, cf. Fig. 8a and d. In the final state of the simulation (cf. Fig. 8), these ions form an extended tail in the ( $y > 0$ ) hemisphere, with the other half space being completely evacuated. Due to their smaller gyroradii, the effect on the macroscopic structure of the pick-up tails formed by the two lighter species is not that pronounced. Inside as well as outside the Saturnian magnetosphere, the  $CH_4^+$  and  $H_2^+$  ion populations are confined to a narrow region between  $y = -2.5 R_T$  and  $y = +2.5 R_T$ , i.e. the overall structure of the corresponding ion tails is not significantly affected. The "mirror effect" due to the nearly complete magnetic field reversal at the magnetopause is well visible in the hydrogen tail structure, cf. Figs. 8c and 9c. Note especially that the dark red contour, denoting the major concentration of hydrogen ions, is shifted from the ( $y < 0$ ) to the ( $y > 0$ )

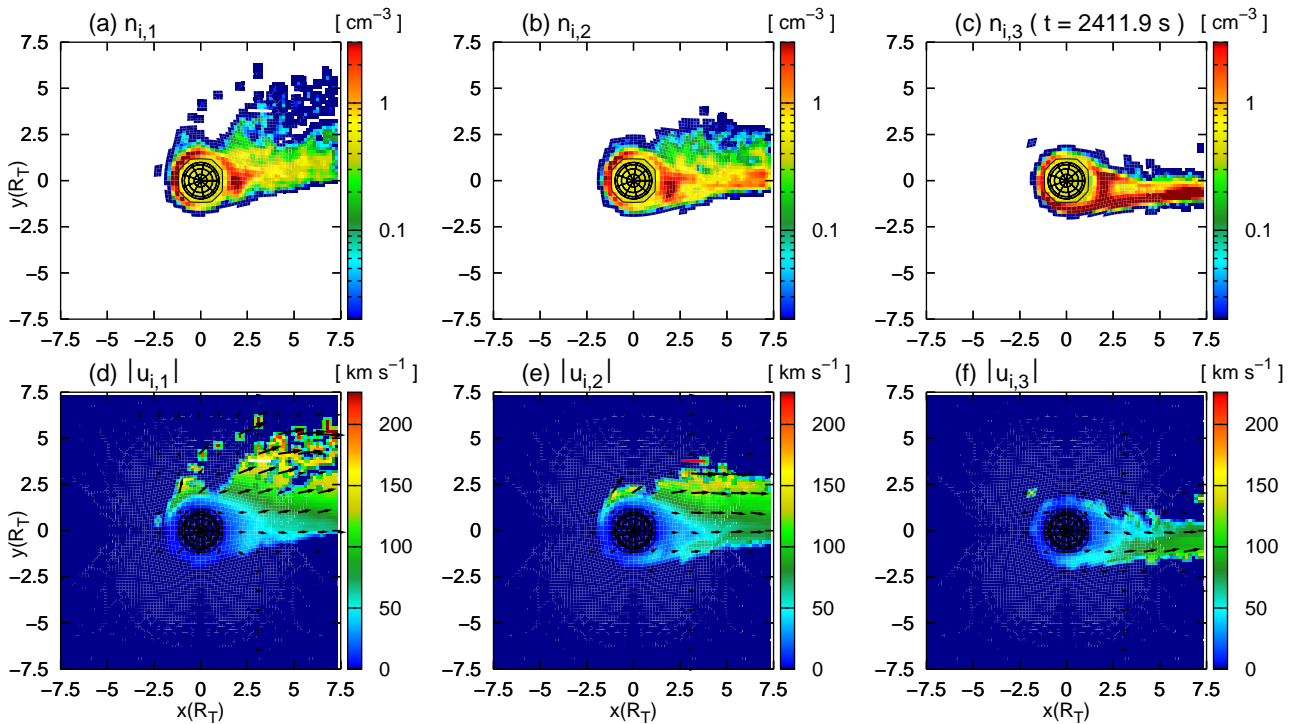


**Fig. 9.** Run # 1. Structure of Titan's ionospheric tail when the moon is located in Saturn's magnetosheath. Since the magnetic  $B_z$  component has reversed its direction at the boundary layer between both plasma regimes, the tail is now shifted in the  $y > 0$  hemisphere. The diameters of the individual tails perpendicular to the undisturbed flow direction provide a rough measure of the corresponding ion mass. The tail is *not* detached from Titan during the passage through the model magnetopause.

half space. The qualitative details of the tail reconfiguration process, especially the influence on particle dynamics, are exactly the same as in the Voyager 1 scenario discussed in our preceding study. Therefore, we have decided not to show a flip-book of the tail reconfiguration again. Instead, we refer the reader to the discussion of run # 5 in the companion work. Finally, it should be noted that the reconfiguration of the tail requires a total duration of about 5 to 6 min, i.e. due to the relatively large mass of the pick-up ions, this process is a little slower than the reconfiguration of the magnetic field topology.

### 3.3 Run # 2: Only hydrogen in magnetosheath

In the second simulation scenario, the plasma inside Saturn's magnetosheath is assumed to consist of light hydrogen ions only. The plasma parameters inside the magnetosphere, on the other hand, are exactly the same as in run # 1. Of course, in the second run, the hydrogen density inside the magnetosheath must be set to a significantly larger value than in run # 1 in order to create a stable boundary layer between both plasma regimes. The mass density in the upstream magnetosheath flow is only about 30% smaller than in run # 1. The key features of Titan's plasma environment inside the magnetosphere are identical to the situation displayed in Fig. 3. After the discontinuity has passed the interaction re-

gion, i.e. after Titan has entered the magnetosheath, the simulation achieves a quasi-stationary state, which is illustrated in Fig. 10. The key elements of the magnetic reconfiguration process are qualitatively the same as shown in the series of snapshots for the first simulation run: The magnetic draping pattern is re-oriented due to reconnection, at first only in the region adjacent to the ramside ionosphere and finally in the distant magnetotail of Titan. The most important result from this simulation run is that the reconfiguration process does not only feature a strong qualitative resemblance to the first scenario under consideration, but there is also a strong quantitative analogy. The characteristic time scales of the reconfiguration process which can be obtained from simulation run # 2 are practically the same as discussed in the previous section. In other words, the composition of the plasma flow inside the magnetosheath does not take a noteworthy influence on the duration of the remagnetization process in Titan's upper ionosphere, despite the different flow patterns of  $O^+$  and  $H^+$  ions (Simon et al., 2007b).

Concerning the magnetic field pattern that is formed after the magnetosheath entry (see Fig. 10c, please note that the same color scale as in the results of run # 1 has been used), there is at least a strong qualitative resemblance to the results obtained from the first simulation scenario. The extension of the wakeside magnetic lobes perpendicular to the flow

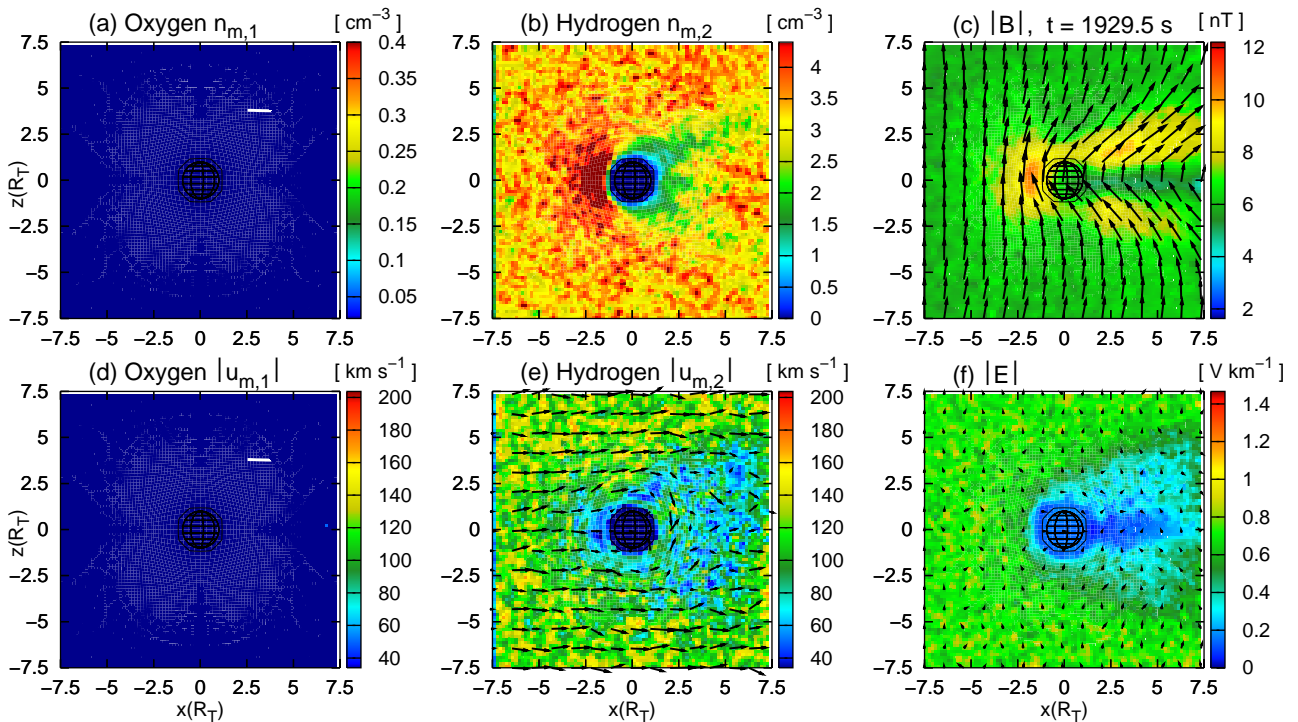


**Fig. 10.** Run # 2. The figure displays the final state of the second model scenario, which assumes the plasma inside Saturn's magnetosheath to consist of light hydrogen ions only. The figure illustrates the structure of Titan's plasma environment after the moon has entered Saturn's magnetosheath. The quantities displayed in the figure are the same as in Fig. 3. Note that the color scale in the hydrogen density plot (b) differs from that used in the first series of simulation results. The magnetic draping pattern qualitatively resembles the results of the first simulation run, although the ramside pile-up region is less compact.

direction as well as the peak magnetic field values achieved in Titan's wakeside magnetotail are only slightly affected by the modified upstream plasma composition. Only the magnetic pile-up region at Titan's ramside features a somewhat different structure. A comparison between Figs. 7c and 10c illustrates that in the second simulation scenario, the magnetic pile-up region is less compact than in the first run. When the magnetosheath plasma consists of hydrogen ions only, a noticeable magnetic field enhancement is already visible at  $x = -4 R_T$ , while in the first scenario, the magnetic field increase commences around the  $x = -2.5 R_T$  line. The absolute field value achieved in the ramside pile-up region is also about 2 nT smaller than in the final state of the first run, applying a two-component representation to the magnetosheath plasma. This can be ascribed to the slightly reduced ram pressure of the magnetosheath plasma in run # 2.

Finally, it should be noted that in the second simulation scenario, Titan's exospheric tail is not detached from the moon either. We have also conducted a test run that uses a hydrogen density of  $n(\text{H}^+) = 1.5 \text{ cm}^{-3}$  for the sheath flow (and no oxygen). Basically, the magnetic reconfiguration scales that can be inferred from such a scenario seem to be the same as in the geometry presented here. However, due to the significant pressure difference between the plasmas upstream

and downstream of the discontinuity, the thin boundary layer between both regimes had already started to change its shape when arriving at Titan's ramside. Therefore, the results obtained from this test run may not be fully reliable with respect to their quantitative relevance.

#### 4 Summary and discussion

Titan, the largest moon of Saturn, orbits the giant planet within the outer regions of Saturn's magnetosphere. Therefore, when Saturn's magnetosphere is compressed due to high solar wind ram pressure, Titan might be able to cross the magnetopause of its parent planet near noon local time and therefore, to interact with the shocked plasma in Saturn's magnetosheath. During the Cassini T32 flyby on 13 June 2007, Cassini became the first spacecraft to conduct in-situ measurements in such a situation. Titan had left the Saturnian magnetosphere only a few minutes before the encounter. Hence, the moon's atmosphere and ionosphere were exposed to a sudden change in the properties of the impinging plasma flow: Cassini magnetometer measurements indicate an almost complete field reversal across the magnetopause discontinuity, while the plasma density also increased dramatically.

Within the framework of the present study, the influence of such sudden changes in the upstream plasma properties on Titan's induced magnetotail has been studied by using a three-dimensional, multi-component hybrid simulation model. Since the hybrid approach treats the involved ion species as individual particles, it is fully applicable to the Titan scenario where the gyroradii of the charged particles are comparable to the spatial extension of the interaction region. The model results presented in this paper are based on a preceding study by the same group of authors (Simon et al., 2008a), investigating the influence of periodic and discontinuous electromagnetic field changes on ion pick-up at Titan. In the simulations presented here, the magnetopause boundary is represented by a thin current sheet, separating two regimes with different plasma and magnetic field characteristics. Two different simulation scenarios have been discussed. In both of them, the magnetic field direction is nearly reversed at the discontinuity, while simultaneously, the field magnitude is reduced. The magnetic field values that have been used as input parameters for the impinging plasma are in agreement with Cassini magnetometer observations during the T32 encounter. In both simulations, the upstream plasma flow inside the magnetosphere is assumed to feature the "classical" Voyager 1 composition, i.e. the flow is made up of hydrogen and oxygen ions, the density ratio being  $n(\text{H}^+):n(\text{O}^+)=1:2$ .

In the first simulation run, the hydrogen density at the upstream side of the current sheet is about a factor of 13 larger than in the downstream region, while the oxygen density is the same on both sides of the discontinuity. The simulations show that when Titan encounters the boundary layer between both plasma regimes, the moon's induced magnetotail is reconfigured due to magnetic reconnection. At first, this process occurs only at the ramside magnetic pile-up region, which is eroded on a characteristic time scale of only a few minutes. Subsequently, Titan's magnetic lobe structure is repolarized due to magnetic merging, the total duration of the reconfiguration process being of the order of only a few minutes again. In general, our results show that the characteristic time scales of the reconnection process are comparable to the convection time of the magnetic field through the interaction region. During the passage of the discontinuity through the interaction region, Titan's exospheric tail changes its orientation due to the magnetic field reversal, but it is not disconnected from the satellite. This result also confirms the findings of our preceding study, which considered neither a change of the impinging plasma composition nor a decrease of the magnetic field magnitude across the discontinuity.

In our second simulation scenario, the plasma in Saturn's magnetosheath was assumed to consist of light hydrogen ions only. The simulation results show that the magnetic reconfiguration process takes place on practically the same time scales as inferred from the first scenario under consideration. Overall, despite some quantitative differences in the structure

of Titan's ramside pile-up region, the magnetic field topology in the interaction region features a strong resemblance to the case of a two-component magnetosheath plasma.

Finally, we shall again mention the constraints of our numerical model. The most critical of them might be that the numerical approach does not allow to consider a change in the direction of the flow velocity across the discontinuity without producing artifacts near the outer boundaries of the simulation box. In the noon region of Saturn's magnetosphere where the T32 flyby took place, the corotating magnetospheric plasma flow is tangential to the magnetopause boundary layer. When the magnetosphere is compressed in times of high solar wind dynamic pressure, the magnetopause might therefore be moving towards Titan in the direction *perpendicular* to the rotating magnetospheric plasma. Of course, the velocity at which the tangential discontinuity travels towards Titan (and which is controlled by the dynamics of the impinging solar wind) certainly differs from the bulk speed of the rotating magnetospheric plasma. The flow pattern inside the magnetosheath might have been completely different from the magnetospheric plasma characteristics as well. Despite the fact that for T32 the required data are still unknown, a hybrid model might not be able to include all of these features into a self-consistent simulation scenario. The simulations presented here represent a first step towards understanding the effects that may have occurred during the T32 magnetopause crossing.

Due to the huge number of unknown parameters, we did not yet succeed in quantitatively reproducing the observations made by the Cassini magnetometer instrument (cf. Fig. 2). Nonetheless, a qualitative comparison to the overall findings of data interpretation (Bertucci et al., 2008) shall be given here. Bertucci et al. (2008) prove that Cassini MAG data show strong hints towards reconnection during the magnetopause passage. In the picture drawn by these authors, Titan opened Saturn's magnetopause like a comet that crosses a sector boundary in the solar wind. This strong analogy is fully confirmed by the results of our simulation study. However, based on the analysis of T32 MAG data, Bertucci et al. (2008) also point out an alternative interpretation of the T32 scenario. This scenario does not include reconnection, but the original draped magnetospheric field lines simply reach the downstream region by slipping around Titan in the third spatial direction (i.e. the  $y$  direction in our model). Our simulation results suggest that the first proposed scenario, which includes reconnection, provides a more realistic description of the T32 flyby.

Nevertheless, comparing our simulation results to the findings of Bertucci et al. (2008) also clearly points out the limitations of the model. According to these authors, part of the magnetic field signature detected between 17:30 UT and 18:00 UT must be ascribed to the presence of *fossil* magnetic fields (Neubauer et al., 2006) in Titan's induced magnetosphere. These field lines originate from Saturn and remained draped around Titan when the moon made its excursion

through the magnetopause boundary. Bertucci et al. (2008) predict a lifetime of these fossil fields between ten minutes and about two hours. As can be seen in our two-dimensional contour plots of the magnetic field, fossil fields that remain in Titan's ramside ionosphere for a long duration after the magnetopause passage are not reproduced by the simulation model. Apart from the unknown flow parameters in the magnetosheath, a major reason for this may be the rather coarse grid resolution of the hybrid model. MHD codes (e.g. Ma et al., 2006) achieve a resolution of less than 50 km, but they fail to reproduce finite gyroradius effects. The hybrid model currently cannot reproduce magnetic fine structures in the ionosphere and therefore, it does not allow to determine the lifetime of possible fossil fields. However, the timescales for the reconfiguration of the overall structure of the interaction region can be obtained from our simulation results. The time scale on which the overall structure of Titan's induced magnetosphere reverses its polarity is controlled by the convection time of the magnetic field in the undisturbed flow at the flanks of the interaction region.

An alternative approach for the T32 scenario might be the multi-fluid approximation. Unlike the MHD codes, these models are able to discriminate between the velocity patterns of different plasma constituents. Recent advances in multi-fluid simulations have allowed to self-consistently simulate the magnetosphere of Saturn with Titan simultaneously orbiting its parent planet (D. Snowden, private correspondence). Such a two-body simulation might be suitable for the T32 scenario, since the compression of Saturn's magnetopause can be self-consistently included by increasing the density of the impinging solar wind plasma flow without altering its velocity. However, a model with such a large computational domain does not only feature a rather rough resolution near Titan, but any kind of fluid-approach would neglect the effects arising from finite ion gyroradii. As discussed in the analysis of run # 1, especially these effects might play a crucial role for understanding the physics of the T32 scenario.

Nevertheless, there may also still be some options for improving the hybrid model description of T32. While being able to cover finite gyroradius effects, none of the existing three-dimensional hybrid codes is capable of providing more than a rather rough and approximative description of Titan's ionosphere. In this region, complex chemical processes might become important, which are so far only covered by the MHD models (Ma et al., 2004, 2006; Ma et al., 2007). Self-consistent description of a possible collisional ionization source is neglected in most of the available models as well. Thus, a first step towards improving the existing T32 model should aim to include some of these effects into the hybrid approach and then, to infer their influence on the time scales of the magnetic reconfiguration process.

*Acknowledgements.* The work of S. Simon and U. Motschmann has been supported by the Deutsche Forschungsgemeinschaft through the grant MO 539/15-1. The work of G. Kleindienst was financially

supported by the German Ministerium für Wirtschaft und Technologie and by the German Aerospace Center (DLR) under grant 50 OH 9901/4.

Topical Editor I. A. Daglis thanks T. E. Cravens for his help in evaluating this paper.

## References

- Backes, H.: Titan's Interaction with the Saturnian Magnetospheric Plasma, PhD thesis, Universität zu Köln, 2005.
- Backes, H., Neubauer, F. M., Dougherty, M. K., Achilleos, N., André, N., Arridge, C. S., Bertucci, C., Jones, G. H., Khurana, K. K., Russell, C. T., and Wennmacher, A.: Titan's Magnetic Field Signature During the First Cassini Encounter, *Science*, 308, 992–995, 2005.
- Bagdonat, T.: Hybrid Simulation of Weak Comets, PhD thesis, Technische Universität Braunschweig, 2005.
- Bagdonat, T. and Motschmann, U.: 3D Hybrid Simulation Code Using Curvilinear Coordinates, *J. Computational Physics*, 183, 470–485, 2002a.
- Bagdonat, T. and Motschmann, U.: From a weak to a strong comet – 3D global hybrid simulation studies, *Earth, Moon Planets*, 90, 305–321, 2002b.
- Bertucci, C., Szego, K., Wahlund, J., Coates, A. J., Neubauer, F. M., Achilleos, N., Arridge, C. S., Dougherty, M. K., and Modolo, R.: Titan in Saturn's Magnetosheath: Cassini MAG Observations During the T32 Encounter, *AGU Fall Meeting Abstracts*, pp. A1022+, 2007.
- Bertucci, C., Achilleos, N., Dougherty, M. K., Modolo, R., Coates, A. J., Szego, K., Masters, A., Ma, Y., Neubauer, F. M., Garnier, P., Wahlund, J.-E., and Young, D. T.: The Magnetic Memory of Titan's Ionized Atmosphere, *Science*, 321, 1475–1478, doi:10.1126/science.1159780, 2008.
- Böswetter, A., Bagdonat, T., Motschmann, U., and Sauer, K.: Plasma boundaries at Mars: a 3-D simulation study, *Ann. Geophys.*, 22, 4363–4379, 2004, <http://www.ann-geophys.net/22/4363/2004/>.
- Böswetter, A., Simon, S., Bagdonat, T., Motschmann, U., Fränz, M., Roussos, E., Krupp, N., Woch, J., Schle, J., Barabash, S., and Lundin, R.: Comparison of plasma data from ASPERA-3/Mars-Express with a 3-D hybrid simulation, *Ann. Geophys.*, 25, 1851–1864, 2007, <http://www.ann-geophys.net/25/1851/2007/>.
- Brecht, S. H., Luhmann, J. G., and Larson, D. J.: Simulation of the Saturnian magnetospheric interaction with Titan, *J. Geophys. Res.*, 105, 13119–13130, 2000.
- Coates, A. J., McAndrews, H. J., Arridge, C. S., Jones, G. H., Crary, F. J., Young, D. T., Szego, K., Sittler, E. C., Thomsen, M. F., Tokar, R. L., Bertucci, C., and Dougherty, M. K.: Titan at Saturn's magnetopause: CAPS results from T32, *AGU Fall Meeting Abstracts*, pp. A1021+, 2007.
- Dougherty, M. K., Kellock, S., Southwood, D. J., Balogh, A., Smith, E. J., Tsurutani, B. T., Gerlach, B., Glassmeier, K.-H., Gleim, F., Russell, C. T., Erdos, G., Neubauer, F. M., and Cowley, S. W. H.: The Cassini Magnetic Field Investigation, *Space Sci. Rev.*, 114, 331–383, doi:10.1007/s11214-004-1432-2, 2004.
- Kallio, E., Sillanpää, I., and Janhunen, P.: Titan in subsonic and supersonic flow, *Geophys. Res. Lett.*, 31, L15703/1–L15703/4,

- doi:10.1029/2004GL020344, 2004.
- Ledvina, S. A., Luhmann, J. G., Brecht, S. H., and Cravens, T. E.: Titan's induced magnetosphere, *Adv. Space Res.*, 33, 2092–2102, 2004.
- Luhmann, J. G.: Titan's ion exosphere wake: A natural ion mass spectrometer?, *J. Geophys. Res.*, 101, 29387–29393, 1996.
- Ma, Y.-J., Nagy, A. F., Cravens, T. E., Sokolov, I. V., Clark, J., and Hansen, K. C.: 3-D global MHD prediction for the first close flyby of Titan by Cassini, *Geophys. Res. Lett.*, 31, 1–4, 2004.
- Ma, Y.-J., Nagy, A. F., Cravens, T. E., Sokolov, I. V., Hansen, K. C., Wahlund, J.-E., Crary, F. J., Coates, A. J., and Dougherty, M. K.: Comparisons between MHD model calculations and observations of Cassini flybys of Titan, *J. Geophys. Res.*, 111, A05207, doi:10.1029/2005JA011481, 2006.
- Ma, Y.-J., Nagy, A. F., Toth, G., Cravens, T. E., Russell, C. T., Gombosi, T. I., Wahlund, J.-E., Crary, F. J., Coates, A. J., Bertucci, C. L., and Neubauer, F. M.: 3D global multi-species Hall-MHD simulation of the Cassini T9 flyby, *Geophys. Res. Lett.*, 34, L24S10, doi:10.1029/2007GL031627, 2007.
- Modolo, R. and Chanteur, G. M.: A global hybrid model for Titan's interaction with the Kronian plasma: Application to the Cassini Ta flyby, *J. Geophys. Res. (Space Physics)*, 113, 1317, doi:10.1029/2007JA012453, 2008.
- Modolo, R., Chanteur, G. M., Wahlund, J.-E., Canu, P., Kurth, W. S., Gurnett, D., Matthews, A. P., and Bertucci, C.: Plasma environment in the wake of Titan from hybrid simulation: A case study, *Geophys. Res. Lett.*, 34, L24S07, doi:10.1029/2007GL030489, 2007.
- Motschmann, U. and Kührt, E.: Interaction of the solar wind with weak obstacles: Hybrid simulations for weakly active comets and for Mars, *Space Sci. Rev.*, 122, 197–208, doi:10.1007/s11214-006-6218-2, 2006.
- Neubauer, F. M., Gurnett, D. A., Scudder, J. D., and Hartle, R. E.: Titan's magnetospheric interaction, in Saturn, edited by T. Gehrels and M. S. Matthews, pp. 760–787, University of Arizona Press, Tucson, Arizona, 1984.
- Neubauer, F. M., Backes, H., Dougherty, M. K., Wennmacher, A., Russell, C. T., Coates, A., Young, D., Achilleos, N., Andre, N., Arridge, C. S., Bertucci, C., Jones, G. H., Khurana, K. K., Knetter, T., Law, A., Lewis, G. R., and Saur, J.: Titan's near magnetotail from magnetic field and plasma observations and modelling: Cassini flybys TA, TB and T3, *J. Geophys. Res.*, 111, A10220, doi:10.1029/2006JA011676, 2006.
- Saur, J. and Strobel, D. F.: Relative contributions of sublimation and volcanoes to Io's atmosphere inferred from its plasma interaction during solar eclipse, *Icarus*, 171, 411–420, 2004.
- Simon, S.: Titan's highly variable plasma environment: A 3D hybrid simulation study, PhD thesis, Technische Universität Braunschweig, 2007.
- Simon, S., Bagdonat, T., Motschmann, U., and Glassmeier, K.-H.: Plasma environment of magnetized asteroids: a 3-D hybrid simulation study, *Ann. Geophys.*, 24, 407–414, 2006a, <http://www.ann-geophys.net/24/407/2006/>.
- Simon, S., Bößwetter, A., Bagdonat, T., Motschmann, U., and Glassmeier, K.-H.: Plasma environment of Titan: a 3-D hybrid simulation study, *Ann. Geophys.*, 24, 1113–1135, 2006b, <http://www.ann-geophys.net/24/1113/2006/>.
- Simon, S., Boesswetter, A., Bagdonat, T., and Motschmann, U.: Physics of the Ion Composition Boundary: a comparative 3-D hybrid simulation study of Mars and Titan, *Ann. Geophys.*, 25, 99–115, 2007a, <http://www.ann-geophys.net/25/99/2007/>.
- Simon, S., Boesswetter, A., Bagdonat, T., Motschmann, U., and Schuele, J.: Three-dimensional multispecies hybrid simulation of Titan's highly variable plasma environment, *Ann. Geophys.*, 25, 117–144, 2007b, <http://www.ann-geophys.net/25/117/2007/>.
- Simon, S., Kleindienst, G., Boesswetter, A., Bagdonat, T., Motschmann, U., Glassmeier, K.-H., Schuele, J., Bertucci, C., and Dougherty, M. K.: Hybrid simulation of Titan's magnetic field signature during the Cassini T9 flyby, *Geophys. Res. Lett.*, 34, L24S08, doi:10.1029/2007GL029967, 2007c.
- Simon, S., Motschmann, U., and Glassmeier, K.-H.: Influence of non-stationary electromagnetic field conditions on ion pick-up at Titan: 3-D multispecies hybrid simulations, *Ann. Geophys.*, 26, 599–617, 2008b, <http://www.ann-geophys.net/26/599/2008/>.
- Simon, S., Motschmann, U., Kleindienst, G., Glassmeier, K.-H., Bertucci, C., and Dougherty, M. K.: Titan's magnetic field signature during the Cassini T34 flyby: Comparison between hybrid simulations and MAG data, *Geophys. Res. Lett.*, 35, L04107, doi:10.1029/2007GL033056, 2008b.
- Snowden, D., Winglee, R., Bertucci, C., and Dougherty, M.: Three-dimensional multifluid simulation of the plasma interaction at Titan, *J. Geophys. Res. (Space Physics)*, 112, 12221, doi:10.1029/2007JA012393, 2007.